Drought prediction Using Deep Learning

Selamawit Kasahun Seifu

A Thesis Submitted to the Department of Computer Science and Engineering

School of Electrical Engineering and Computing

Office of Graduate Studies

Adama Science and Technology University

September, 2024

Adama, Ethiopia

Drought prediction Using Deep Learning

Selamawit Kasahun Seifu

Advisor**:** Worku J. (Assoc. Prof)

A Thesis Submitted to the Department of Computer

Science and Engineering

School of Electrical Engineering and Computing

Office of Graduate Studies

Adama Science and Technology University

September, 2024

Adama ,Ethiopia

Declaration

I declare that this thesis/dissertation proposal entitled **“Drought prediction Using Deep Learning”** is my work and has not been submitted to any university for a similar purpose. The references used in this proposal are duly recognized by proper citations.

____________________	____________________	____________________
Name of student	Signature	Date

Advisor Recommendation

I the advisor of this research Paper, hereby certify that I have closely advised the student while developing this Research and read the draft thesis/dissertation proposal entitled **“Drought prediction Using Deep Learning”** prepared under my guidance by **Selamawit Kasahun Seifu**. Therefore, I recommend the submission of the Thesis to the department for further review and evaluation.

______________________	________________________	__________________
Advisor/Supervisor	Signature	Date

Approval Page for Advisor

I/we here by certify that the recommendation and suggestion given by the proposal review committee are appropriately incorporated into the final thesis/dissertation proposal entitled "**Drought prediction Using Deep Learning**" by **Selamawit Kasahun Seifu**.

________________	________________	____________
Advisor/ Supervisor	Signature	Date

Approval of Board of Reviewers

We, the undersigned, members of the Board of Reviewers of the proposal open defense by Selamawit Kasahun Seifu have read and evaluated the thesis/dissertation proposal entitled "**Drought prediction Using Deep Learning**" and assessed the understanding of the candidate about the proposed research. This is, therefore, to certify that the thesis/dissertation proposal is accepted and we recommend the implementation of the proposal.

________________	________________	________________
Chairperson	Signature	Date
________________	________________	________________
Reviewer 1	Signature	Date
________________	________________	________________
Reviewer 2	Signature	Date

Final approval and acceptance of the thesis/dissertation proposal is contingent upon submission of its final copy to the Office of Postgraduate Studies (OPGS) through the Department Graduate Council (DGC) and School Graduate Committee (SGC).

________________	________________	________________
Department Head	Signature	Date
________________	________________	________________
School Dean	Signature	Date
________________	________________	________________
Office of Postgrad	Signature	Date

ACKNOWLEDGMENT

First of all, I would like to thank almighty of God and his Mother Saint Mary for guiding me and supporting me though out this MSc thesis. This work comes in to end not only by the effort of the researcher but also the support of many individuals and organizations. To begin with, I would like to thank Dr Worku.J (Assoc. Prof), my advisor, for his constructive suggestions throughout my work. Had it been without his support, this work would not have been come in to reality.

Secondly, my heartfelt thanks to my family to unwavering support and encouragement throughout my MSc journey.

Finally I would like to thanks to Ethiopian National Metrology Agency for their support to providing me the necessary data to conduct this MSc thesis.

Table of Contents

LIST OF TABLES

LIST OF FIGURES

List of Acronyms

AI	Aridity Index.
ANN	Artificial Neural Network.
ARIMA	Auto-Regressive Integrated Moving Average.
Bi-LSTM	Bidirectional LSTM.
CMI	Crop Moisture Index.
CNN	Convolutional Neural Networks.
ConvLSTM	Convolutional LSTM.
DRI	Drought Reconnaissance Index.
HTC	Hydro-thermal Coefficient of Selyaninov.
KBDI	Keetch-Byram Drought Index.
LSTM	Long Short Term Memory.
MAE	Mean Absolute Error.
MPE	Mean Percentage Error.
MSE	Mean Squared Error.
NDVI	Normalized Difference Vegetation Index.
PDSI	Palmer Drought Severity Index.

PET	Potential evapotranspiration.
PET	Weighted Anomaly Standardized Precipitation.
ReLU	Rectified Linear Unit.
RNN	Recurrent Neural Network.
SDI	Standardized Drought Index.
SPEI	Standardized Precipitation Evapotranspiration Index
SPI	Standardized Precipitation Index.
SVM	Support Vector Machines

ABSTRACT

Drought is a complex natural disaster that will directly impact human living status, not only the living status of individuals but also the economic status. The best prediction of whether there is a drought in the upcoming seasons or not is important for effective water resource management and agricultural planning. This study presents analysis of various methods to drought prediction using Convolutional Neural Networks (CNN) and Long Short Term Memory (LSTM) based approaches. We utilized a model to forecast rainfall, maximum temperature, and minimum temperature, which are critical indicators of drought conditions. The study leverages the strengths of Artificial Neural Network to estimate and predict drought for specific regions.

The deep learning model was trained and validated with an extensive dataset that includes over 30 years of monthly records for precipitation, maximum temperature, and minimum temperature from various geographical locations. Based on these forecasts, we utilize the Standardized Precipitation Evapotranspiration Index (SPEI) to predict drought conditions. Our evaluation of various LSTM-based models, including Vanilla LSTM, Stacked LSTM, Bidirectional LSTM, Stacked Bidirectional LSTM, CNN- LSTM, and Conv LSTM, revealed that the Vanilla LSTM and Conv LSTM models performed best for short-term predictions, especially for SPEI-3, achieving high scores in accuracy, precision, recall, and F1- **measure.** *Still, all models showed a decline in performance for longer timescales* **demonstrating** *the challenge of maintaining accuracy over extended period.*

Keywords: - ***Drought, Prediction, Deep Learning***

CHAPTER ONE

1. INTRODUCTION

1.1. Background

Drought is a natural hazard defined by an extended period of insufficient rainfall, resulting insignificant water shortages in the affected regions. It impacts agriculture, water supply, and the environment, creating challenges for both human and ecological systems. Unlike other natural disasters, droughts develop gradually and can persist for months or even years making them particularly challenging to predict and manage. The complexity of drought lies in its various definitions meteorological, agricultural, hydrological, or socio-economic—each emphasizing different facets of the issue. Accurate prediction of drought conditions is essential for effective water resource management and agricultural planning, helping to mitigate the negative effects on society. In recent years, advancements in drought prediction have emerged through improved data collection, computational power, and modeling techniques, offering promising prospects for earlier drought detection. Traditional methods, such as statistical models and hydrological simulations, utilize historical weather data to forecast future drought conditions. Recently, many studies have increasingly adopted machine learning and deep learning methods due to their capacity to manage large datasets and identify complex patterns based on previous data models like support vector machines (SVM), random forests, and artificial neural networks (ANN) have demonstrated effectiveness in various studies. Additionally, remote sensing technologies provide valuable real-time predictions. Notably, the integration of convolutional neural networks (CNN) and long short-term memory (LSTM) networks, known as CONV-LSTM models, has emerged as a powerful approach for drought prediction. These models leverage the spatial feature extraction strengths of CNNs along with the temporal sequence learning capabilities of LSTMs, making them particularly suitable for analyzing climate data. Moreover, techniques like the standardized precipitation evapotranspiration index (SPEI) and other indexing methods are commonly employed to quantify drought severity and duration, offering a standardized means to assess and compare drought conditions across different regions and time period.

1.2. Motivation

The motivation for using deep learning to predict drought stems from the urgent need to mitigate its impacts on various sectors, including agriculture, water resource management, and climate resilience. Droughts can lead to severe consequences such as crop failures, water shortages, and ecological disruptions, causing significant economic and social upheaval. Traditional methods of drought prediction often depend on limited data and simplistic models that struggle to capture the complex and evolving nature of drought patterns. By leveraging deep learning capabilities, we can enhance prediction accuracy and gain a better understanding of drought dynamics. Deep learning algorithms can uncover hidden patterns and relationships within large datasets, facilitating more precise and timely drought forecasts. This study aims to develop robust and reliable drought prediction models that will support effective management strategies and assist decision-makers in reducing drought impacts. In certain regions of Ethiopia, particularly in the Oromia Regional State (Borena Zone) and parts of the Somali Regional State, drought has affected communities in multiple ways. This issue drives our research to predict droughts before they cause significant harm and to identify measures to lessen their effects on community livelihoods.

Deep learning algorithms have the potential to provide valuable insights and comparisons in drought prediction. We will conduct a comprehensive evaluation of these algorithms' applicability and effectiveness in forecasting drought conditions. Consequently, we propose utilizing deep learning algorithms to anticipate droughts based on specific drought indicators.

1.3. Problem Statement

Drought has significant effects across various sectors and regions, leading to serious social, economic, and environmental consequences. It can reduce crop yields, cause livestock losses, and increase the vulnerability of rural communities in agricultural areas. Water shortages due to drought compromise supplies for drinking, sanitation, and industry, threatening public health and hindering economic activities. Ecosystems are also affected, as reduced water availability can lead to habitat degradation, species displacement, and loss of biodiversity. Additionally, drought heightens the risk of wildfires, accelerates soil erosion, and threatens hydropower generation. The socioeconomic impacts include job losses, decreased incomes, rising food prices, and increased migration pressures. Given these extensive repercussions, effective forecasting and timely management of drought through advanced techniques like deep learning could help mitigate its effects and enhance resilience in affected regions. Previous research on drought prediction has faced challenges in selecting suitable indicators for accurate forecasting, securing high-quality data for training deep learning models, and tackling the complex nature of drought events. Earlier efforts using machine learning and deep learning methods have encountered limitations in these areas (Brust et al., 2021; Gyaneshwar et al., 2023; Mei et al., 2022; Raja & Gopikrishnan, 2022). To overcome these challenges, this study suggests employing deep learning algorithms to proactively predict and forecast drought conditions, allowing for early detection and intervention before severe impacts occur. Recently, the Oromia region, especially the Borena zone, has been significantly impacted by drought, highlighting the need for reliable prediction methods.

Figure 1: Drought in the Borena zone is said to have killed over three million cattle (Photo: SM)

1.4. Research Question

RQ1. What are variables that are used to predict the drought?

RQ2. What are better deep learning model used to predict and forecast drought?

RQ3. What are the next five years drought prediction in some selected site of Ethiopia?

1.5. Objectives

1.5.1. General Objective

The general objective of this research is to utilizing a deep learning Model that predict Droughts in some selected area of Ethiopia.

1.5.2. Specific Objective

- Identify variables that are used to predict drought with deep learning model

- Select a better deep learning model that better predict the availability of drought in Ethiopia

- Predict the next five years regarding the availability of drought in Ethiopia

1.6. Significance

The importance of utilizing deep learning to anticipate drought episodes stems from its ability to improve our understanding and preparedness for drought disasters. Deep learning approaches can analyze big and complicated datasets effectively, allowing the detection of detailed patterns and relationships within meteorological data. This data is critical for policymakers, water resource managers, farmers, and communities to conduct proactive water management, agricultural planning, and resource allocation initiatives.

Accurate drought forecasting allows for early warning systems, allowing for appropriate interventions and adaptive techniques to lessen the effects of drought. We can improve our ability to respond effectively to drought occurrences, reduce economic losses, protect ecosystems, and assure the sustainability of water resources by adding deep learning into drought prediction.

1.7. Scope and Limitation

Today, there are numerous types of methods are available for predicting drought. However, this study will only look at predicting drought using deep learning approach.

CHAPTER TWO
2. LITERATURE REVIEW

2.1. Overview of Drought

Drought is a complex and multi-dimensional natural occurrence defined by extended durations of below-normal rainfall, resulting in substantial water shortages. It is not simply a lack of moisture; rather, it arises from the interaction between natural climate fluctuations and human water consumption, which can worsen the effects of drought. The American Meteorological Society (AMS) highlights that drought is a transient aspect of the climate cycle that can cause severe repercussions for agriculture, ecosystems, and economies worldwide.

Drought is a prolonged period of abnormally low rainfall that leads to significant water shortages, impacting agriculture, water supply, and ecosystems (State of California Department of Water Resources, 2017). It can be driven by climatic variability, such as changes in weather patterns, as well as human activities like deforestation and over extraction of water resources (United Nations Office for the Coordination of Humanitarian Affairs, 2011). The consequences of drought include agricultural losses, water shortages, economic instability, and environmental degradation, which can threaten food security and biodiversity (Australian Bureau of Meteorology, 2010). Effective management strategies, including water conservation practices and the development of drought-resistant crops, are essential for mitigating the impacts of drought and enhancing resilience in affected regions (World Bank, 2020).

2.2. Deep learning

Deep learning is a type of machine learning and artificial intelligence (AI) that imitates the way humans gain certain types of knowledge. Deep learning models can be taught to perform classification tasks and recognize patterns in photos, text, audio and other various data. It is also used to automate tasks that would normally need human intelligence, such as describing images or transcribing audio files.

Deep learning is an important element of data science, including statistics and predictive modeling. It is extremely beneficial to data scientists who are tasked with collecting, analyzing and interpreting large amounts of data; deep learning makes this process faster and easier.

2.3. Literature Review

Drought happens in both high and low rainfall locations. It is a situation relative to some long term average condition of balance between rainfall and Evapotranspiration in a given area, a condition generally viewed as 'normal'. However, average rainfall is rarely an acceptable statistical measure of rainfall features in a given location, particularly in dry places. (Wilhite & Glantz, 1985).

Drought poses a threat to water and food security, to every water-use sector, and thus to livelihoods, in virtually every climate zone. In recent years, a number of major droughts have revealed the vulnerability of even wealthy societies to drought and caused conflicts among water users. Drought can perturb the environment, at least temporarily, with a reduction in ecosystem condition and resilience and a loss of ecosystem services. With climate projections suggesting that droughts will intensify in many regions the magnitude of drought and associated impacts is likely to increase. At the same time, drought is an elusive phenomenon that differs substantially from other natural hazards, making its management a challenging task. First, it is a slowly developing hazard without a distinct onset and end; second, it is not precisely and universally defined. Third, drought is multifaceted, affecting different parts of the hydrological cycle, ecosystems, and sectors of society; and fourth, impacts of drought are often nonstructural and difficult to quantify or monetize. (Bachmair et al., 2016).

The paper "A Deep Learning Based Approach for Long-Term Drought Prediction" by Norbert Agana and Abdollah Homaifar (2017), explores the application of a Deep Belief Network (DBN) for predicting drought conditions in the Gunnison River Basin. The authors highlight the complexity of drought as a natural disaster characterized by a significant deficit in precipitation, which affects various water-related resources and has far-reaching consequences. This underscores the need for reliable predictive models to aid in drought management. The proposed model consists of two Restricted Boltzmann Machines (RBMs) stacked to form the DBN, utilizing lagged values of the Standardized Stream flow Index (SSI) as inputs. The methodology involves several steps, including obtaining different time scale SSIs (e.g., SSI 12 and SSI 24), normalizing the data, splitting it into training and testing sets, initializing the DBN parameters, pre-training the DBN using unsupervised learning, fine-tuning the network with the back-propagation algorithm, and testing the model. The study compares the performance of the DBN against traditional forecasting methods, such as Multi-Layer Perceptron (MLP) and Support

Vector Regression (SVR). The results indicate that the DBN consistently achieves lower prediction errors, as measured by metrics like Root Mean Square Error (RMSE) and Mean Absolute Error (MAE). The DBN model demonstrates superior predictive skill, particularly for the SSI 24 forecasts, which show improved accuracy over the SSI 12 forecasts. Visual comparisons of the predicted and observed SSI values for all three models illustrate the effectiveness of the DBN. Its ability to handle complex, nonlinear relationships in the data contributes to its enhanced performance. The paper concludes that the DBN is a promising approach for long-term drought prediction, offering significant advantages over traditional methods. Furthermore, the authors suggest that future work could explore integrating global climate indices with the DBN model to further improve prediction accuracy.

The study titled "Drought Prediction: A Comprehensive Review of Different Drought Prediction Models and Adopted Technologies" provides an in-depth examination of the complexities surrounding drought prediction. It begins by highlighting the significant impact of droughts on human life and economies, emphasizing the challenges posed by their unpredictable nature. The authors, Neeta Nandgude and colleagues(2023), conducted a thorough review of 131 research articles, focusing on various drought prediction models, including statistical methods and advanced machine learning techniques. The review discusses the integration of technologies such as remote sensing and geographic information systems (GIS) to enhance the accuracy of drought predictions. It also addresses the challenges faced in this field, such as data limitations and the need for improved methodologies. The authors suggest that future research should focus on developing more reliable models and fostering collaboration among researchers, policymakers, and stakeholders to better manage drought risks. In conclusion, the article serves as a comprehensive resource for understanding the current landscape of drought prediction research, the technologies employed, and the future directions needed to improve drought management strategies. Drought happens in both high and low rainfall locations. It is a situation relative to some long-term average condition of balance between rainfall and Evapotranspiration in a given area, a condition generally viewed as 'normal'. However, average rainfall is rarely an acceptable statistical measure of rainfall features in a given location, particularly in dry places. (Wilhite & Glantz, 1985).

Drought poses a threat to water and food security, to every water-use sector, and thus to livelihoods, in virtually every climate zone. In recent years, a number of major droughts have revealed the vulnerability of even wealthy societies to drought and caused conflicts among water users. Drought can perturb the environment, at least temporarily, with a reduction in ecosystem condition and resilience and a loss of ecosystem services. With climate projections suggesting that droughts will intensify in many regions the magnitude of drought and associated impacts is likely to increase. At the same time, drought is an elusive phenomenon that differs substantially from other natural hazards, making its management a challenging task. First, it is a slowly developing hazard without a distinct onset and end; second, it is not precisely and universally defined. Third, drought is multifaceted, affecting different parts of the hydrological cycle, ecosystems, and sectors of society; and fourth, impacts of drought are often nonstructural and difficult to quantify or monetize.(Bachmair et al., 2016).

This study provides a comprehensive analysis of drought in Hawaiʻi over the past century (1920-2019) using a newly developed gridded Standardized Precipitation Index (SPI) dataset. The authors categorize drought effects into five types: meteorological, agricultural, hydrological, ecological, and socioeconomic. Findings reveal significant increases in drought duration and magnitude, primarily linked to El Niño events, with notable droughts occurring between 1998-2002 and 2007-2014.

The paper emphasizes the substantial economic impacts of drought, including over $80 million in agricultural relief since 1996, and increased wildfire risks, especially during El Niño years. It calls for enhanced understanding of drought dynamics to inform effective resource management and policy development, particularly in light of anticipated climate changes that may exacerbate drought conditions in the future. The work serves as a framework for analyzing drought in other tropical island systems with complex topography.

The paper develops a deep learning model combining Gated Recurrent Units (GRU) and Convolutional Neural Networks (CNN) to predict the Monthly Meteorological Composite Index (MCI) drought index in Yunnan Province, China. Utilizing historical meteorological data from 1960 to 2020, the model significantly outperformed traditional methods like LASSO and Random Forest. The findings underscore the importance of accurate drought prediction for effective climate-risk management in the region.

Table 1: Summary of Related works

Title	Authors	Methodology	Key Findings	Gaps Identified
A Deep Learning Based Approach for Long-Term Drought Prediction	Norbert A Agana, Abdollah Homaifar (2017)	Deep Belief Network (DBN) with two Restricted Boltzmann Machines (RBMs) using Standardized Stream flow Index (SSI)	DBN achieves lower prediction errors than traditional methods (MLP and SVR), Especially for SSI 24.	Limited exploration of external climate factors influencing drought patterns.
Drought Prediction: A Comprehensive Review of Different Drought Prediction Models and Adopted Technologies	Neeta Nandgude et al. (2023)	Review of 131 research articles focusing on various drought prediction models and technologies	Highlights the impact of droughts; discusses the role of remote sensing and GIS in predictions.	Lack of consensus on best practices and comprehensive methodologies across studies.
Understanding Drought Dynamics	Wilhite & Glantz (1985)	Discusses the relative nature of drought, focusing on rainfall and evapotranspiration balance	Drought is multifaceted, affecting various sectors; challenges in defining and managing drought are highlighted.	Insufficient focus on socio-economic impacts and quantification of nonstructural effects.
Drought Management Challenges	Bachmair et al. (2016)	Analysis of drought management complexities in relation to climate change and ecosystem impacts	Drought management is challenging due to its slow Development, multifaceted nature, and difficulty in quantifying impacts.	Need for integrated approaches considering environmental and socio-economic factors.

Drought Analysis)	Hawai‘i (1920-2019)	Analyzes a gridded Standardized Precipitation Index (SPI) dataset, categorizing drought effects	Significant increases in drought duration/magnitude linked to El Niño; economic impacts exceed $80 million in agricultural relief.	Limited examination of long-term mitigation strategies for affected sectors.
Deep Learning for Drought Prediction in Yunnan Province	Ping Mei (1960 - 2020)	Combines Gated Recurrent Units (GRU) and Convolutional Neural Networks (CNN) for Monthly Meteorological Composite Index (MCI)	Model outperforms traditional methods (LASSO, Random Forest) in predicting drought; emphasizes importance for climate risk management.	Need for validation of model performance across different geographical regions and climates.

CHAPTER THREE

3. METHODOLOGY

In this study, we developed several LSTM models integrated with Convolutional Neural Networks (CNN) to assess their effectiveness in predicting drought conditions. The outputs from each model are utilized to calculate the Standardized Precipitation Evapotranspiration Index (SPEI). This section will outline the specifics of each model's architecture and the meteorological standardized drought indices.

3.1. Model Architectures

3.1.1. Long Short Term Memory (LSTM)

Long Short Term Memory (LSTM) networks, created by SeppHochreiter and Jürgen Schmidhuber in 1997, are a specialized form of Recurrent Neural Network (RNN) that overcome the challenges of traditional RNNs, such as vanishing and exploding gradients. LSTMs excel at learning and retaining long-term dependencies in sequential data, thanks to their distinctive architecture, which includes memory cells and gating mechanisms (input, forget, and output gates).The LSTM network [Figure 2] comprises several essential components that facilitate the capture of long-term dependencies in sequential data: the forget gate, input gate, cell state, and output gate. The Long Short Term Memory (LSTM) network [Figure2] consists of several key components that allow it to effectively capture long-term dependencies in sequential data. These components are the forget gate, input gate, cell state, and output gate.

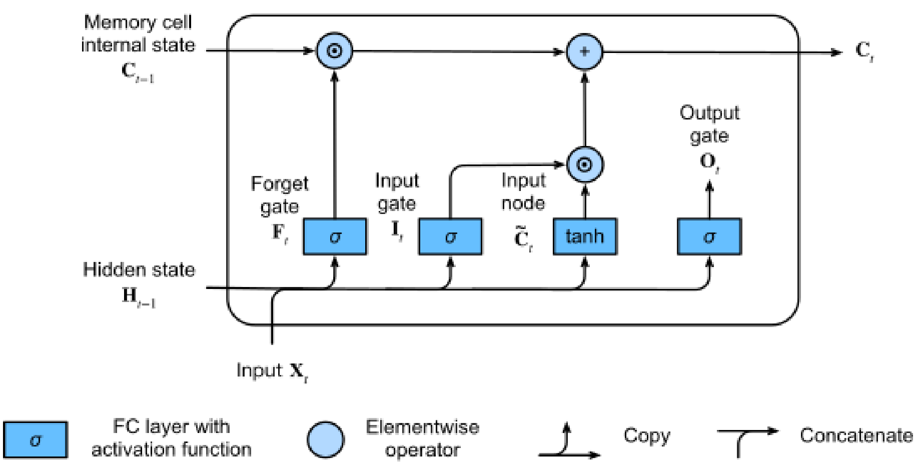

Figure 2: Architecture of a LSTM Unit.

The forget gate determines which information is discarded from the cell state. It employs a sigmoid activation function that produces a value between 0 and 1, where 0 signifies complete removal and 1 indicates total retention. The formula for the forget gate is:

Defined as $\boldsymbol{f(x) = \sigma(Wf.[ht-1, xt] + bf)}$ Eq. (1)

Where σ is the sigmoid function, $\boldsymbol{W_f}$ is the weight matrix, $\boldsymbol{h_{t-1}}$ is the previous hidden state, $\boldsymbol{x_t}$ is the current input, and b_f is the bias. The sigmoid function is

Defined as $\boldsymbol{\sigma\ (x) = 1 + \frac{1}{e-x}}$ Eq. (2)

The **input gate** determines what new information to add to the cell state. It also uses a sigmoid function to decide which values to update, combined with a tan h function to create a vector of new candidate values, $\tilde{C}t$ that could be added to the state. The formulas are:

$$\boldsymbol{it = \sigma(Wi \cdot [ht-1, xt] + bi)} \quad \text{Eq. (3)}$$

$$\tilde{C}t = \tanh\ (W_C \cdot [h_{t-1}, x_t] + b_C) \quad \text{Eq. (4)}$$

Here, W_i and W_C are weight matrices, b_i and b_C are biases. The tanh function is

Defined as:

$$\boldsymbol{\tanh\ (x) = \frac{ex - e-x}{ex + e-x}} \quad \text{Eq. (5)}$$

The **cell state** C_t is updated based on the forget gate and the input gate. The forget gate controls which information from the previous cell state C_{t-1} should be retained, and the input gate updates the cell state with the new candidate values $\tilde{C}t$. The cell state is updated using the following formula:

$$\boldsymbol{Ct = ft \cdot Ct-1 + it \cdot \tilde{C}t} \quad \text{Eq. (6)}$$

The **output gate** determines the output of the LSTM unit. It uses a sigmoid function to decide which parts of the cell state should be output, combined with the tan h function applied to the cell state to limit the values between -1 and 1. The formulas are:

$$\boldsymbol{ot = \sigma(Wo \cdot [ht-1, xt] + bo)} \quad \text{Eq. (7)}$$

$$ht = ot \cdot \tanh(Ct) \qquad \text{Eq. (8)}$$

Here, W_o is the weight matrix, b_o is the bias, and h_t is the hidden state, which serves as the output of the LSTM cell. There is a multiple variant of LSTM model, for this study, we will cover the following models.

Vanilla LSTM is a basic LSTM model with a single hidden layer of LSTM units and an output layer used to make predictions. Its simplicity lies in using one layer to capture long-term dependencies in sequential data. This straight sequences sequentially, updating hidden and cell states at each step. Forward architecture processes input

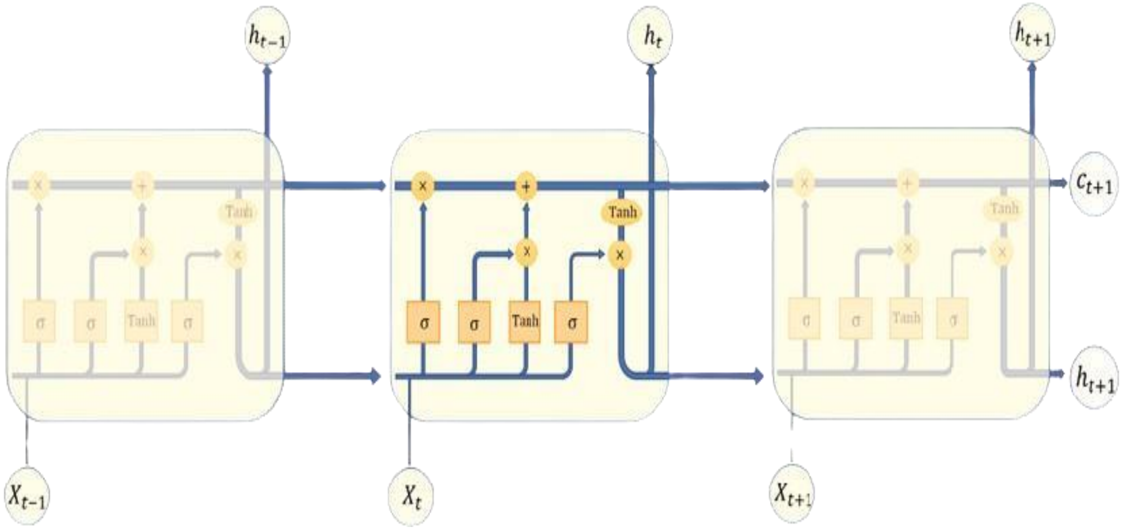

Figure 3: Architecture of Vanilla LSTM

Stacked LSTM is an enhanced version of the basic LSTM architecture, comprising several LSTM layers stacked sequentially. This configuration allows the model to capture and represent more intricate temporal patterns and dependencies in sequential data. Each LSTM layer processes the output sequences from the layer before it, enabling the network to develop progressively abstract and high-level features.

Stacked Bidirectional LSTM is made up of multiple layers of bidirectional LSTM units, with each bidirectional layer handling the combined output from the layer before it.

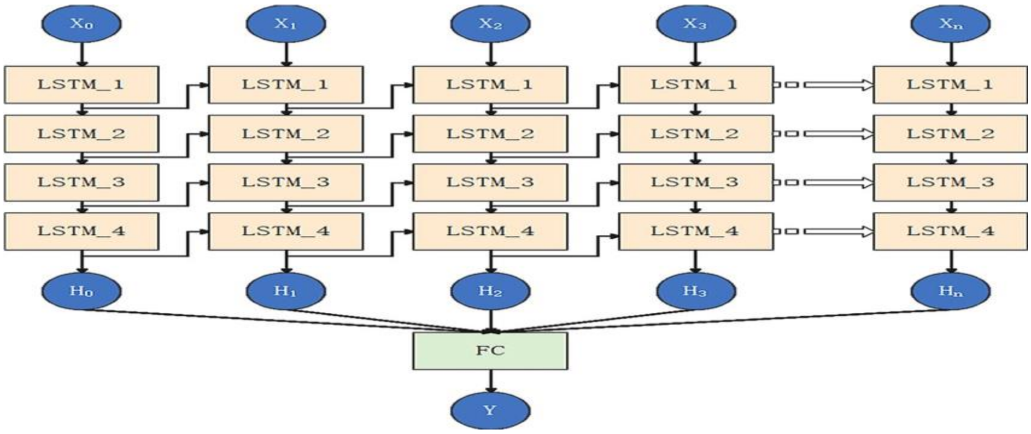

Figure 4: Architecture of Stacked LSTM

Bidirectional LSTM (**Bi-LSTM**) is a type of LSTM network that analyzes data in both forward and backward directions, enabling it to collect information from both past and future contexts at the same time**.**

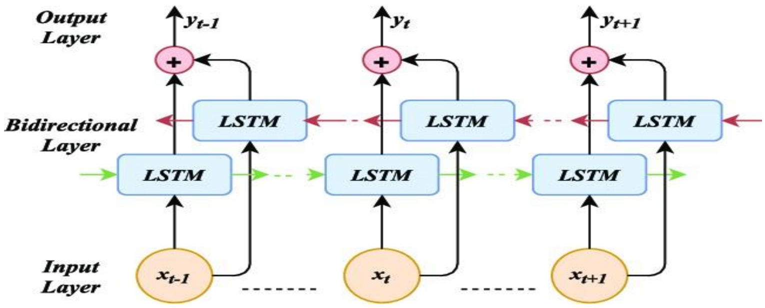

Figure 5: Architecture of Bi-LSTM

3.2. Convolutional Neural Network (CNN)

Convolutional Neural Networks (CNN) is a type of deep learning model is used to analyze visual data. Its architecture is inspired by the visual cortex of animals, and it is particularly effective for image and video recognition tasks. CNNs are com-posed of several key layers, each with a specific role in processing and understanding the input data.

The **Convolutional Layer** is the first essential component of a CNN. It applies a set of filters (kernels) to the input image, performing convolution operations to produce feature maps. These feature maps capture various patterns such as edges, textures, and shapes at different locations in the input image. The convolution operation involves sliding the filter over the input and computing dot products between the filter and patches of the input. To introduce non-linearity into the model, CNNs utilize activation functions, with the **Rectified Linear Unit (ReLU)** being the most common.

The ReLU function applies an element-wise operation, converting all negative values in the feature maps to zero while keeping positive values unchanged. After convolution and activation, the network typically includes a **Pooling Layer**, which reduces the spatial dimensions of the feature maps. Pooling operations, such as max pooling, take the maximum value from patches of the feature map, effectively down sampling the data. This reduction in size helps decrease the number of parameters, mitigates over fitting, and makes the network invariant to small translations and distortions in the input image.

CNNs also contain **Fully Connected Layers** (or **Dense Layers**) towards the end of the architecture. These layers take the high-level feature maps generated by the convolutional and pooling layers and interpret them to make a final decision or prediction.

Each neuron in a fully connected layer is connected to every neuron in the previous layer. An essential aspect of CNNs is the **Flattening** operation, which converts the 2D feature maps into a 1D vector before passing them to the fully connected layers. This transformation is necessary because the dense layers expect a 1D input, and it allows the network to combine spatial features learned in previous layers.

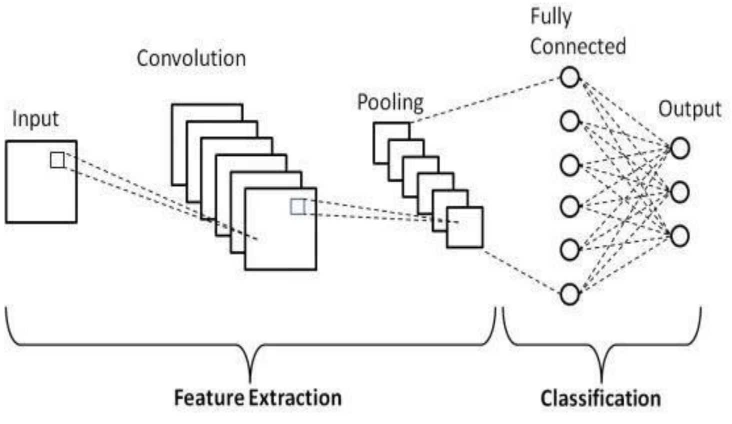

Figure 6: Architecture of CNN model

3.3. Types of LSTM Models for Time Series Forecasting

Univariate LSTM models are specifically created for time series data involving a single variable predicted from its historical values. These models are effective for forecasting one time-dependent variable by identifying patterns in its past data. A common application of univariate LSTM models is predicting future stock prices based on historical stock prices.

Multivariate LSTM models build on the univariate approach by managing multiple variables at once. These models forecast one or more dependent variables using historical data from several related time series. For instance, in weather forecasting, a multivariate LSTM could predict temperature by considering past values of temperature, humidity, pressure, and wind speed.

Multi-step LSTM models are structured to predict several future time steps simultaneously, instead of only forecasting the immediate next time step.

Multivariate multi-step LSTM models combine the capabilities of multivariate and multistep LSTM models. They predict multiple future time steps of one or more dependent variables using historical data from multiple time series. This type of model is particularly useful in complex scenarios such as climate modeling, where the aim might be to predict various either conditions (temperature, humidity, etc.) over the next several days based on multiple past observations.

3.3.1. Hybrid of CNN and LSTM models

CNN-LSTM Combining Convolutional Neural Networks (CNN) and Long Short Term Memory (LSTM) networks can be particularly effective for predicting droughts, as these models can leverage both spatial and temporal data features. Here are the main ways to integrate CNNs and LSTMs for drought prediction:

Using the Output of the CNN as the Input to the LSTM in this method, the CNN processes spatial data, such as satellite images or spatial cli- mate data, to extract features. These extracted features are then flattened and fed in to the LSTM, which models the temporal dependencies to predict future drought conditions.

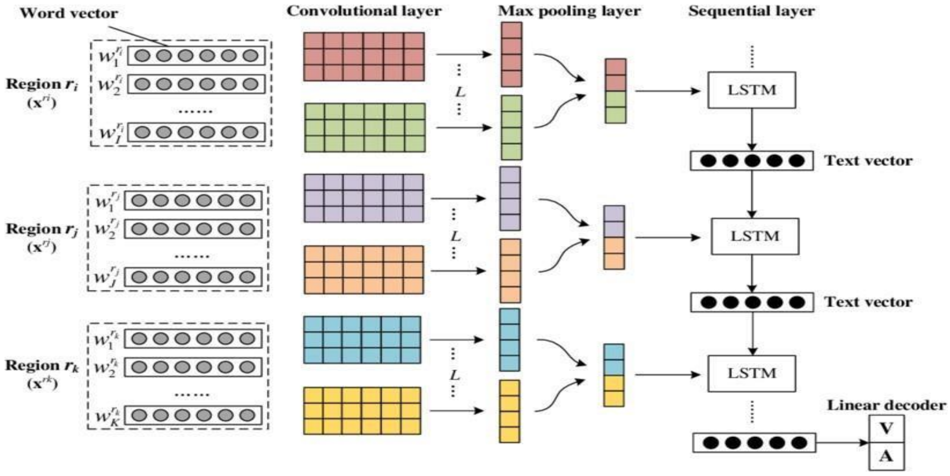

Figure 7: Architecture of CNN-LSTM hybrid model

Example: For drought prediction, satellite images of vegetation indices (such as NDVI) are processed by the CNN to extract spatial features. These features are then passed to the LSTM, which uses past time steps to predict future drought events.

Using the Output of the LSTM as the Input to the CNN In this approach, the LSTM first processes sequential data, such as time series of climate variables, and generates output sequences that are then fed into the CNN. This method can be useful when it is essential to model temporal dynamics before extracting spatial patterns.

Example: Climate data time series, including variables like temperature and precipitation, are first processed by the LSTM to capture temporal patterns. The output sequences from the LSTM are then input into the CNN to extract spatial patterns that are significant for predicting droughts.

Parallel Architecture with CNN and LSTM Operating Independently in this architecture, both CNN and LSTM operate on the input data independently. The outputs from both networks are then concatenated and passed to a fully connected layer. This method allows the model to capture both spatial and temporal features simultaneously and can be particularly powerful for complex tasks.

Example: For drought prediction, satellite images are processed by the CNN to extract spatial features, while time series data of climatic variables are processed by the LSTM to capture temporal dependencies. The outputs of both networks are concatenated and fed into a fully connected layer to predict drought conditions.

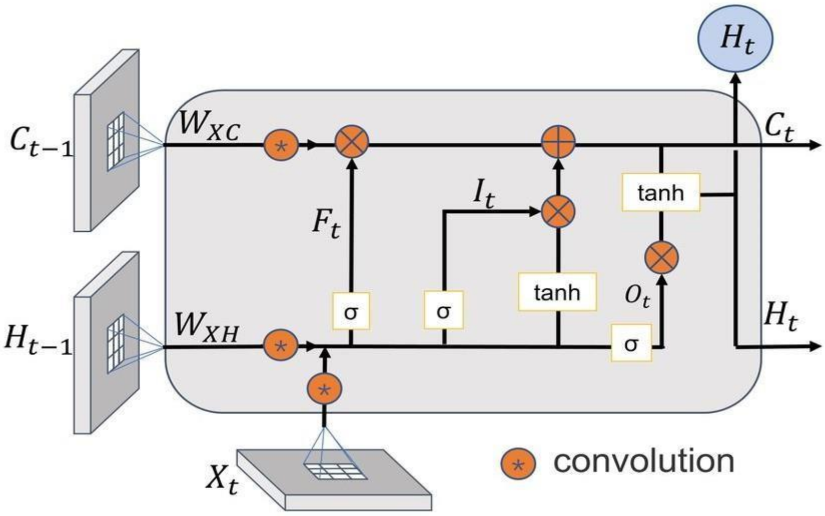

Figure 8: Architecture of ConvLSTM

3.3.2. Convolutional LSTM

Convolutional LSTM (ConvLSTM) is an advanced neural network architecture that merges the strengths of Convolutional Neural Networks (CNN) and Long Short Term Memory (LSTM) networks into a single model. This hybrid architecture is particularly well-suited for tasks involving spatiotemporal data, where both spatial and temporal patterns need to be captured and analyzed. ConvLSTM models are employed in a variety of applications, including weather forecasting, video analysis, and environmental monitoring, to leverage both spatial and temporal dependencies in the data. ConvLSTM models address the challenge of handling spatially and temporally correlated data by incorporating convolutional operations within the LSTM units. In traditional LSTM networks, the input, output, and state transitions are managed through fully connected layers, which are not ideal for spatial data. ConvLSTM replaces these fully connected layers with convolutional layers, enabling the model to maintain the spatial structure of the data while learning temporal dependencies. This is crucial for applications such as video analysis and weather prediction, where the spatial relationships within the data are just as important as the temporal sequences. In ConvLSTM, the input to each cell is a sequence of frames, and the convolutional operations are applied to these frames to extract spatial features at each time step. The recurrent nature of LSTM cells then captures the temporal dependencies across these frames. This combination allows ConvLSTM to effectively model the spatiotemporal dynamics present in the data.

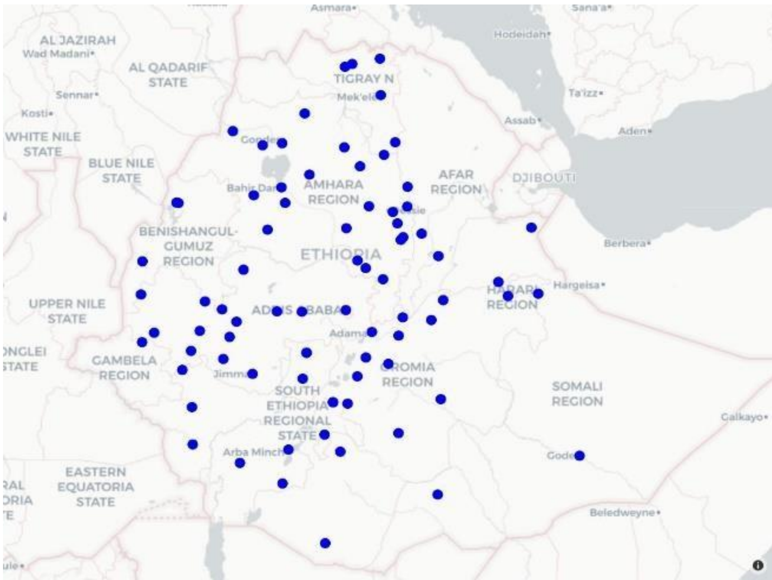

Figure 9: Data distribution across Ethiopian locations

One of the key applications of ConvLSTM is in weather forecasting, particularly for tasks such as precipitation now casting. In this context, ConvLSTM models process sequences of radar images to predict short-term weather conditions, such as rainfall intensity and movement. The convolutional layers extract spatial features from the radar images, while the LSTM layers capture the temporal evolution of these features to make accurate forecasts. The structure of a ConvLSTM cell includes gates that control the flow of information into and out of the cell, similar to traditional LSTM cells. However, these gates use convolutional operations to process the data, preserving the spatial structure.

3.4 Data Collection

In this study, we have used monthly meteorological data from Ethiopian National Meteorology Agency. The data includes the precipitation and temperature data of 76 cities and 80 geographical sites in Ethiopia. The dataset contains 12 months of data on monthly maximum temperature, minimum temperature, and precipitation. The selection site was based on the geographical location of the country, namely north, south, east and west. It was hard to include all sizes across the country, so we have used to consider samples from the four geographical location. The following are all columns provided with the dataset:

- ✓ *NAME* - The legal location name.
- ✓ *YEAR* - The year in which the climate element is recorded.
- ✓ *GH ID* - Unique identifier of the meteorological site.
- ✓ *GEOGR1* - The geographical latitude of the meteorological site.

- ✓ *GEOGR2* - The geographical longitude of the meteorological site.
- ✓ *ELEVATION* - Elevation of the specified location.
- ✓ *Element* - Type of climate data

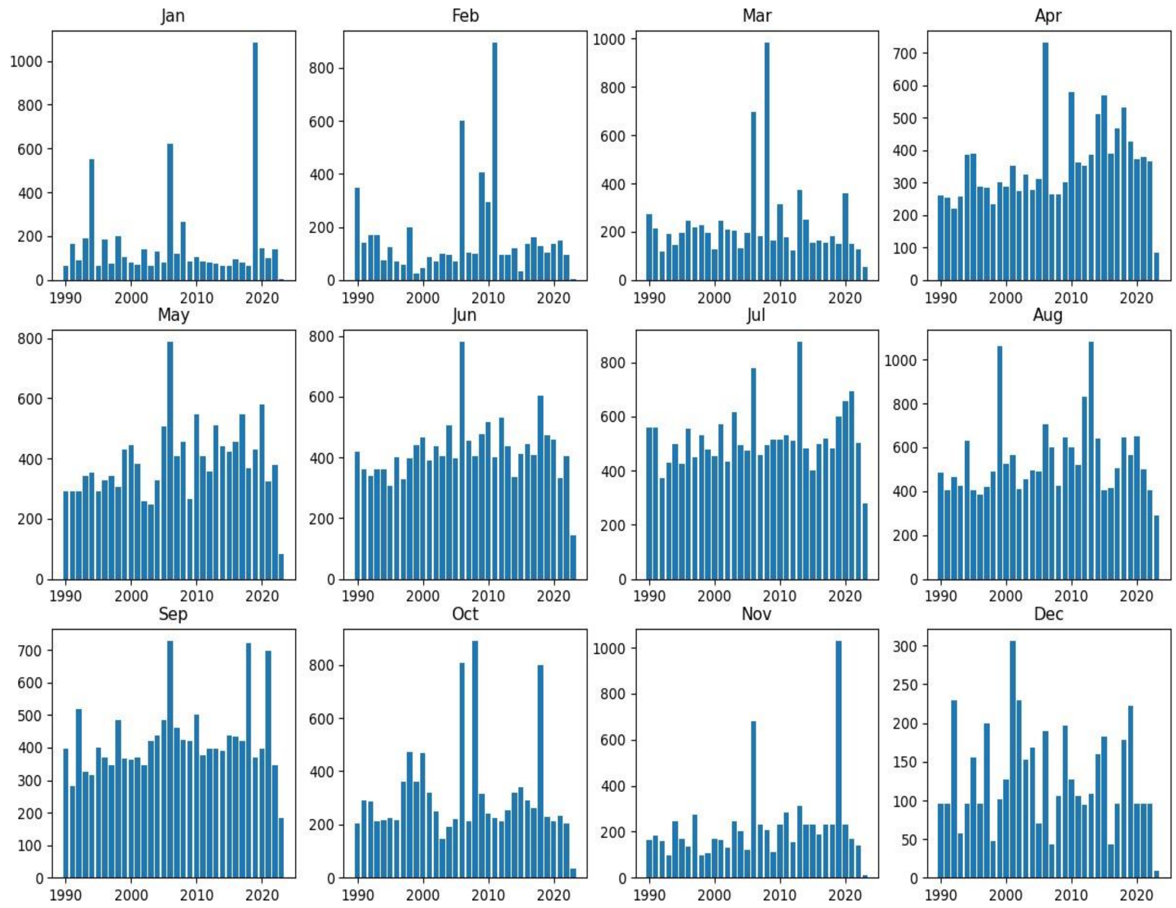

Precipitation data over the year

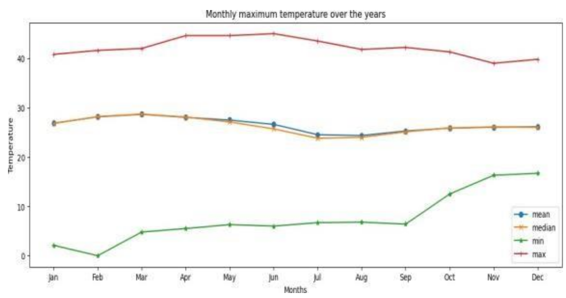

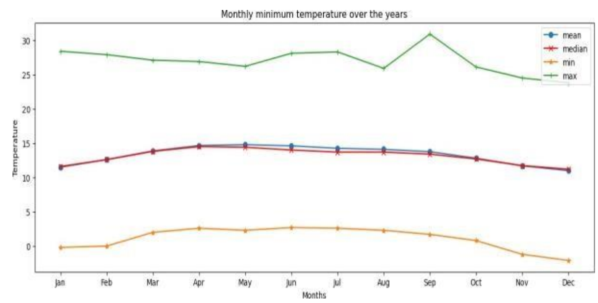

Maximum and minimum temperature data over the years

Figure 10: Monthly data distribution over the years

- *PRECIP* - Precipitation information of specified year for each month *TMPMIN* - The minimum information recorded per month for the year.
- *TMPMAX* - The maximum information recorded per month for the year.

Months from *January* to *December* with the value of the specified element.

3.5. Data Pre-processing

The first step in building a machine learning model is pre-processing the given data. In our case, the data is organized in a tabular format, with each row representing a data point for a specific year, geographical location, and climate element. The data is collected from multiple geographical locations in the Ethiopia region. We have performed the following data-cleaning steps: The analysis of the average distance between working sites of one state is very close across the country, which gives us an insight into filling the missing geographical points (latitude and longitude) with the equidistant relative to the surrounding sites. Having the geographical coordinates, and filling in the missing elevation data is straightforward. We find the actual elevation data using dCode.fr API. The statistical measurements of the data distribution, displayed in figure 10, indicate the majority of the data points are accumulated into the center of the data. This helps us to decide how we handle the missing data on an average group of climate data. The data was organized in a way that each row represents a climate element of a specific region in a specific year. The data will be incomplete if one of the elements is missing for a specific year. We drop rows with incomplete elements. In addition, we dropped a row with a meteorological site of data less than 180 months which is not enough to accomplish a time series forecasting.

3.5. Feature Engineering

After cleaning the data, the next step was making the data good for feature extraction which will help the LSTM learn from the time series data, so the model can forecast the next maximum temperature, minimum temperature, and monthly precipitation for prediction of drought. The first step of our feature engineering was converting the given dataset into a time series format by transposing the columns of months into rows and putting the climate elements as columns with site ID and other locations. After this, we will have a time series data sorted by year and the information for each year. We select all three elements as a future due to the reason that different standardized drought indices use different outputs [8].

Table 1: Modified dataset columns.

NAME	GH_ID	GEOGR2	GEOGR1	ELEVATION	Element	YEAR	Jan	Feb	Mar	Apr	May	Jun
Adet	GOADET11	11.2745	37.49312	2179	PRECIP	1990	2	3.3		23.8	59.2	104.3
Adet	GOADET11	11.2745	37.49312	2179	PRECIP	1991	0					344.1
Adet	GOADET11	11.2745	37.49312	2179	PRECIP	1992	0	0	30.5	138.7	33.7	62.4
Adet	GOADET11	11.2745	37.49312	2179	PRECIP	1993	0	36	43.1	57.4	187.2	70.4
Adet	GOADET11	11.2745	37.49312	2179	PRECIP	1994	0	16	10.6	25.2	173.5	203.1
Adet	GOADET11	11.2745	37.49312	2179	PRECIP	1995	0	0	34.6	36.2	135.2	153.8
Adet	GOADET11	11.2745	37.49312	2179	PRECIP	1996	6.2	2.5	95.1	165.8	174.2	205.1
Adet	GOADET11	11.2745	37.49312	2179	PRECIP	1997	3.4	0	48.9	20.2	247.3	158.6
Adet	GOADET11	11.2745	37.49312	2179	PRECIP	1998	2.5	0	23.5	19.7	182	155.1
Adet	GOADET11	11.2745	37.49312	2179	PRECIP	1999	26.3	0	1.7	24.1	95.8	131.4
Adet	GOADET11	11.2745	37.49312	2179	PRECIP	2000	0		2.4	134.9	58.7	99.6
Adet	GOADET11	11.2745	37.49312	2179	PRECIP	2001	0	4.1	2.7	34.1	136.9	193.7
Adet	GOADET11	11.2745	37.49312	2179	PRECIP	2002	11.7	3.8	39.2	35.6	50.5	136
Adet	GOADET11	11.2745	37.49312	2179	PRECIP	2003	0	7.9	10.1	6.1	16.2	162.7
Adet	GOADET11	11.2745	37.49312	2179	PRECIP	2004	7.7	7	2	36.9	10.2	189.3
Adet	GOADET11	11.2745	37.49312	2179	PRECIP	2005	1.7	0	27.9	40.4		105.1
Adet	GOADET11	11.2745	37.49312	2179	PRECIP	2006	0	0.8	4.3	19	116.4	175
Adet	GOADET11	11.2745	37.49312	2179	PRECIP	2007	3.5	1	14.1	19.7	94.3	271.9
Adet	GOADET11	11.2745	37.49312	2179	PRECIP	2008	15.1	1	0	168.2	150.6	142.6
Adet	GOADET11	11.2745	37.49312	2179	PRECIP	2009	0	10.9	34.7	32.6	46	100.7
Adet	GOADET11	11.2745	37.49312	2179	PRECIP	2010	22.5	0	0	44.7	78.6	160
Adet	GOADET11	11.2745	37.49312	2179	PRECIP	2011	21.2	0	23.9	70.5	161.6	83.6
Adet	GOADET11	11.2745	37.49312	2179	PRECIP	2012					35	177.6
Adet	GOADET11	11.2745	37.49312	2179	PRECIP	2013	0.1	0	11	5.7	112.7	157.6
Adet	GOADET11	11.2745	37.49312	2179	PRECIP	2014	0	3.5	114.2	85.6	188.3	130.6
Adet	GOADET11	11.2745	37.49312	2179	PRECIP	2015	0	1.8	22.3	0.8	139.3	141.7
Adet	GOADET11	11.2745	37.49312	2179	PRECIP	2016	0	2.5	73.8	21.4	201.2	161
Adet	GOADET11	11.2745	37.49312	2179	PRECIP	2017	0	40.9	17.7	121.9	110.5	80
Adet	GOADET11	11.2745	37.49312	2179	PRECIP	2018	0	0	37.9	15.8	107.3	159.9

The time series data alone is not effective in describing the climate pattern. So we grouped the data based on their specific site id (*GH ID*, so the model can learn pattern from the long-range specific location.

3.6. Model Training

3.6.1. Evaluation Metrics

We are developing a forecasting model to estimate essential climate factors like precipitation, maximum temperature, and minimum temperature. The main goal is to utilize these predictions for precise drought forecasting. To assess the model's effectiveness, we use Mean Squared Error

(MSE) as the evaluation metric for both the training and validation losses. The MSE is computed as follows: The formula for Mean Squared Error (MSE) is:

$$\mathbf{MSE} = \frac{\mathbf{1}}{\boldsymbol{n}} \sum_{\boldsymbol{i=1}}^{\boldsymbol{n}} (\mathbf{yi} - \boldsymbol{y}\text{^}\mathbf{i})\ \mathbf{2} \qquad \text{Eq. (9)}$$

Where *n* is the number of observations, *yi* is the actual value, i*y^i* is the predicted value.

The Mean Absolute Error (MAE) is a metric used to evaluate the accuracy of a predictive model by measuring the average magnitude of errors in a set of predictions. It is defined as follows

$$\mathbf{MAE} = \frac{\mathbf{1}}{\boldsymbol{n}} \sum_{\boldsymbol{i=1}}^{\boldsymbol{n}} |\mathbf{yi} - \boldsymbol{y}^{\mathbf{i}}|\ \mathbf{2} \qquad \text{Eq. (10)}$$

In addition to MSE, we also compare the results based on Mean Absolute Error (MAE) and Mean Percentage Error (MPE). The MAE is given by and the MPE is

Defined as:

$$\mathbf{PE} = \frac{\mathbf{1}}{\boldsymbol{n}} \sum_{\boldsymbol{i=1}}^{\boldsymbol{n}} \frac{(\boldsymbol{yi} - \boldsymbol{y}\text{^}\mathbf{i})}{\boldsymbol{yi}} \boldsymbol{x}\mathbf{100}) \qquad \text{Eq. (11)}$$

Our models are used to predict data for 3, 6, 9, and 12 months into the future. Based on these predictions, we calculate the Standardized Precipitation Evapotranspiration Index (SPEI) and classify drought severity. After obtaining the SPEI values, we compare the labeled drought conditions with the actual results. Based on this comparison, we compute various performance metrics, including total accuracy, precision, recall, and the F1-score. Mathematically the metrics are defined as follows:

$$\mathbf{Accuracy} = \frac{\boldsymbol{TP+TN}}{\boldsymbol{TP+TN+FP+FN}} \qquad \text{Eq. (12)}$$

$$\text{Precision} = \frac{\boldsymbol{TP}}{\boldsymbol{TP+FP}} \qquad \text{Eq. (13)}$$

$$\mathbf{F1 - Score} = \mathbf{2\,x} \frac{\boldsymbol{PrecisionxRecall}}{\boldsymbol{Precision+Recall}} \qquad \text{Eq. (14)}$$

Where TP, TN, FP, and FN represent true positives, true negatives, false positives, and false negatives, respectively. By evaluating each approach using these metrics, we aim to identify the most accurate and reliable forecasting model for drought prediction.

3.6.2. Standardized Drought Indices

The Standardized Drought Index (SDI) is a general term that can refer to any drought index standardized to enable comparisons across different regions and timescales. It often involves normalizing variables like precipitation and temperature. SDI provides a common framework for drought assessment, facilitating regional and temporal comparisons, and can be applied to various drought indices. SDI is useful for comparative studies and regional drought monitoring where standardization is necessary. In our study, we evaluated several drought indices that utilize both precipitation (P) and temperature (T) to determine their effectiveness for drought prediction. The indices considered include Standardized Precipitation Evapotranspiration Index (SPEI), Keetch-Byram Drought Index (KBDI) Weighted Anomaly Standardized Precipitation (PET), Aridity Index (AI), Crop Moisture Index (CMI), and Drought Reconnaissance Index (DRI).

Standardized Precipitation Evapotranspiration Index (SPEI) Incorporates both precipitation and temperature data to calculate evapotranspiration and assess the balance between water input and output. SPEI captures the impact of temperature on drought conditions and can be computed over various timescales, allowing for flexibility in assessing both short-term and long term droughts. However, it requires a serially complete dataset for both temperature and precipitation, which may limit its use in regions with insufficient data. Standardized Precipitation Evapotranspiration Index (SPEI) is particularly useful for identifying the impact of climate change on drought by considering the effects of increasing temperatures.

The Drought Reconnaissance Index (DRI) includes a simplified water balance equation considering precipitation and PET. It has three outputs: the initial value, the normalized value, and the standardized value, which can be directly compared to SPI. DRI is more representative than SPI because it considers the full water balance instead of precipitation alone. However, PET calculations can be Subject to errors when using temperature alone, and monthly timescales may not react quickly enough for rapidly developing droughts.

The Hydro-thermal Coefficient of Selyaninov (HTC) uses temperature and precipitation values and is sensitive to dry conditions specific to the climate regime being monitored. It is flexible enough to be used in both monthly and decadal applications. HTC is simple to calculate and the values can be applied to agricultural conditions during the growing season. However, the calculations do not take into account soil moisture, which limits its comprehensiveness in drought assessment.

The Keetch-Byram Drought Index (KBDI) uses daily maximum temperature and daily precipitation to monitor fire danger due to drought. It calculates moisture deficiency in the upper layers of the soil and indicates the amount of precipitation needed to saturate the soil. KBDI is useful for both fire danger and agricultural contexts, as it expresses moisture deficiency and is simple to use. How- ever, it assumes a limit of available moisture and requires specific climatic conditions for drought to develop.

The Weighted Anomaly Standardized Precipitation (PET) index utilizes gridded precipitation and temperature data to monitor drought in tropical regions. PET is valuable for its use of gridded data, making it effective for large- scale drought monitoring. However, it may not be as effective in regions with sparse data availability.

The Aridity Index (AI) is often used in climate classifications and considers both precipitation and temperature data. Aridity Index (AI) helps in understanding the balance between precipitation and evapotranspiration, providing insights into arid and semi-arid conditions. However, it may not be suitable for detailed drought monitoring due to its broader application in climate classification.

The Crop Moisture Index (CMI) is calculated weekly and uses weekly precipitation and mean temperature. It responds quickly to changing conditions, making it suitable for monitoring short-term agricultural droughts. However, it was developed specifically for grain-producing regions and may not accurately reflect long-term drought conditions. Among the indices reviewed, the Standardized Precipitation Evapotranspiration Index (SPEI) stands out due to its comprehensive incorporation of temperature effects alongside precipitation, providing a balanced approach to understanding water Availability and drought severity.

Its flexibility across different timescales makes it particularly advantageous for comprehensive drought assessment. These indicators are often used to provide a comprehensive understanding of drought conditions and their impacts on different sectors. Among those tools when we have maximum and minimum temperature and precipitation data, the Standardized Precipitation Evapotranspiration Index (SPEI) [1] is a particularly good drought indicator.

The SPEI combines the sensitivity of PDSI to changes in evaporation demand (caused by temperature fluctuations and trends) with the simplicity of calculation and the multi-temporal nature of the SPI. The SPI cannot identify the role of temperature increase in future drought conditions, and independently of global warming scenarios cannot account for the influence of temperature variability and the role of heat waves.
The SPEI can account for the possible effects of temperature variability and temperature extremes beyond the context of global warming.

Two reasons why SPEI is good for our case:

- **Temperature Inclusion**: Unlike the Standardized Precipitation Index (SPI), the SPEI incorporates temperature data, which allows it to account for the effects of temperature on water balance. Higher temperatures increase evapotranspiration, which can exacerbate drought conditions.

- **Comprehensive Assessment**: SPEI combines both precipitation and potential evapotranspiration (PET), providing a more holistic measure of drought by considering the water demand in addition to the water supply.

All the needed element for calculating SPEI is provided by our trained model. After calculating SPEI if the result is an indicator of wetter than average but if is negative the value indicates drier than average. How are we going to calculate SPEI with the given data, we calculate SPEI with those three elements. The SPEI uses the monthly (or weekly) difference between precipitation and PET. This represents a simple climatic water balance which is calculated at different time scales to obtain the SPEI. With a value for PET, the difference between the precipitation (P) and PET for the month i is calculated.

$$\boldsymbol{PETi = 10.Ti^2} \qquad \text{Eq. (15)}$$

Where: PETi = Potential Evapotranspiration for period ii (mm/day) Ti = Average temperature during period ii (°C) a = A constant that changes depending on climate or empirical data (typically between 2 & 3) the empirical exponent a in your formula can be calculated using the following polynomial expression based on temperature T:

The equation for (a) is given by: $6.75\times10^{-7}T^{3} - 7.71\times10^{-5}T^{2} + 1.792\times 10^{-2}T + 0.49239$.

$$\mathbf{Di = Pi - PETi} \qquad \text{Eq. (16)}$$

Selection of the most suitable statistical distribution to model the D series was difficult, given the similarity among the four distributions (Pearson III, Lognormal, Log-logistic and General Extreme Value). The selection was based on the behavior at the most extreme values. Log logistic distribution showed a gradual decrease in the curve for low values, and coherent probabilities were obtained for very low values of D, corresponding to 1 occurrence in 200 to 500 years. Additionally, no values were found below the origin parameter of the distribution.

$$\boldsymbol{f(x) = \frac{ß.(x-\gamma)1^{ß-1}}{\delta^{\delta}.(x-\gamma)1^{ß-2}}} \qquad \text{Eq. (17)}$$

Where α, β and γ are scale, shape and origin parameters, respectively, for D values in the range ($\gamma > D < \infty$). Parameters of the Log-logistic distribution can be obtained following different procedures. Among them, the L-moment procedure is the most robust and easy approach (Ahmad et al., 1988). When L-moments are calculated, the parameters of the Log logistic distribution can be obtained following Singh et al. (1993):

$$\boldsymbol{\beta = \frac{2W1-W0}{6W1-W0-6W2}} \qquad \text{Eq. (18)}$$

$$\boldsymbol{\alpha = (W0 - 2W1)\beta} \qquad \text{Eq. (19)}$$

$$\boldsymbol{\gamma = w - \alpha\Gamma\left(1+\frac{1}{\beta}\right)\left(1-\frac{1}{\beta}\right)} \qquad \text{Eq. (20)}$$

Where Γ (β) is the gamma function of β.In Vicente-Serrano et al. (2010), when the log-logistic α,β and γ distribution parameters were calculated, the probability-weighted moments (PWMs) method was used, based on the plotting-position approach (Hosking, 1990), where the PWMs of order s are calculated as:

$$\boldsymbol{Ws} = \frac{\mathbf{1}}{\boldsymbol{N}}\sum_{\boldsymbol{i}=\mathbf{1}}^{\boldsymbol{N}}(\mathbf{1} - \boldsymbol{Fi})^{\boldsymbol{s}}\,\boldsymbol{Di} \qquad \text{Eq. (21)}$$

Where *N* is the number of data, F_i is a frequency estimator following the approach of Hosking (1990) and D_i is the difference between Precipitation and Potential Evapotranspiration for the month *i*. Nevertheless, we have found that using the plotting position formulae the standard deviation of the SPEI series changes noticeably as a function of the SPEI time scale, which affects the spatial comparability of the SPEI values. On the contrary, if the PWMs are obtained using the unbiased estimator given by Hosking (1986), the SD of the series does not change among the different SPEI time scales. The unbiased PWMs are obtained according to:

$$\boldsymbol{Ws} = \frac{\mathbf{1}}{\boldsymbol{N}}\sum_{\boldsymbol{i}=\mathbf{1}}^{\boldsymbol{N}}(\mathbf{1} - \boldsymbol{Fi})^{\boldsymbol{s}+\mathbf{1}}\,\boldsymbol{Di} \qquad \text{Eq. (22)}$$

The method also solves the problem of the no solution of the SPEI model in some regions of the world. For these reasons, we recommend SPEI calculation using unbiased PWMs. The probability distribution function of *D* according to the Log-logistic distribution is then given by:

$$\boldsymbol{F}(\boldsymbol{x}) = (\mathbf{1} + (\frac{\boldsymbol{\alpha}(\boldsymbol{x}-\boldsymbol{\gamma})}{\boldsymbol{\beta}})^{-\mathbf{1}})^{-\mathbf{1}} \qquad \text{Eq. (23)}$$

With *F* (*x*) the SPEI can easily be obtained as the standardized values of *F* (*x*). For example, following the classical approximation of Abramowitz and Stegun (1965):

$$\boldsymbol{SPE1} = \boldsymbol{C0} + \boldsymbol{C1W} + \boldsymbol{C2W}^{\mathbf{2}} - (\boldsymbol{W} - \mathbf{1} + \boldsymbol{d1W} + \boldsymbol{d2W}^{\mathbf{2}} + \boldsymbol{d3W}^{\mathbf{3}} \qquad \text{Eq. (24)}$$

$$\boldsymbol{W} = -\mathbf{2ln}(\boldsymbol{P}) \qquad \text{Eq. (25)}$$

For $P \leq 0.5$, P being the probability of exceeding a determined D value, $P = 1 - F(x)$ If $P > 0.5$, P is replaced by $1 - P$ and the sign of the resultant SPEI is reversed. The constants are: $C_0 =$ 2.515517, $C_1 = 0.802853$, $C_2 = 0.010328$, $d_1 = 1.432788$, $d_2 = 0.189269$, $d_3 =$ 0.001308. The average value of the SPEI is 0, and the standard deviation is 1.

The SPEI is a standardized variable, and it can therefore be compared with other SPEI values over time and space. An SPEI of 0 indicates a value corresponding to 50% of the cumulative probability of *D*, according to a Log-logistic distribution. After completing the calculation, the result can be used to classify drought sensitivity. Table 2 shows available ranges for classification.

Table 2: SPEI Ranges and Drought Categories

SPEI Range	Drought Category
SPEI ≥ 2.0	Extremely Wet
1.5 ≤ SPEI < 2.0	Very Wet
1.0 ≤ SPEI < 1.5	Moderately Wet
-1.0 < SPEI < 1.0	Near Normal
-1.5 ≤ SPEI ≤ -1.0	Moderately Dry
-2.0 ≤ SPEI < -1.5	Severely Dry
SPEI < -2.0	Extremely Dry

3.6.3. Experiment Setup

We have adjusted different hyper parameters to effectively configure and train LSTM models for drought prediction. One key parameter is the number of previous time steps used to predict the next one, set to 3, 6, 9, 12, and 24 based on the number of months need to be predicted. The target variables, including precipitation, maximum temperature, and minimum temperature, define the specific outputs the model is framed to predict, shaping the configuration of the output layer accordingly.

In addition to the target variables, the input features used for prediction are also specified, such as precipitation, maximum temperature, and minimum temperature. The proportion of data allocated for training, typically set at 90% or 80%, ensures that the model has sufficient data to learn from while reserving a portion for testing to allow robust evaluation. A normalization step, using a scalar, is crucial for standardizing the data so that all features contribute equally to the learning process and prevent any single feature from dominating due to scale differences. The model iterates over the entire training dataset one hundred times, allowing for thorough learning. The batch size, often set to 32 or 1, dictates the number of samples processed before updating the model's parameters, balancing computational efficiency and convergence speed. A validation split, set at 10%, ensures that a portion of the training data is used for validation, helping to monitor the model's performance and avoid over fitting. To further enhance training efficiency, we use callbacks such as early stopping and learning rate reduction.

3.7. Model Components

In this study, we used several LSTM-based models are used for drought prediction, each with distinct components and configurations tailored to capture temporal dependencies and improve prediction accuracy.

Vanilla LSTM model is designed with simplicity and effectiveness in mind. It includes a single LSTM layer with 100 units, which processes input sequences to capture temporal dependencies. Following this, the model flattens the output to prepare it for the dense layers. The model includes two dense layers, each with 128 units and ReLU activation functions, interspersed with Dropout layers to prevent over fitting. The final output is reshaped to match the required prediction format.

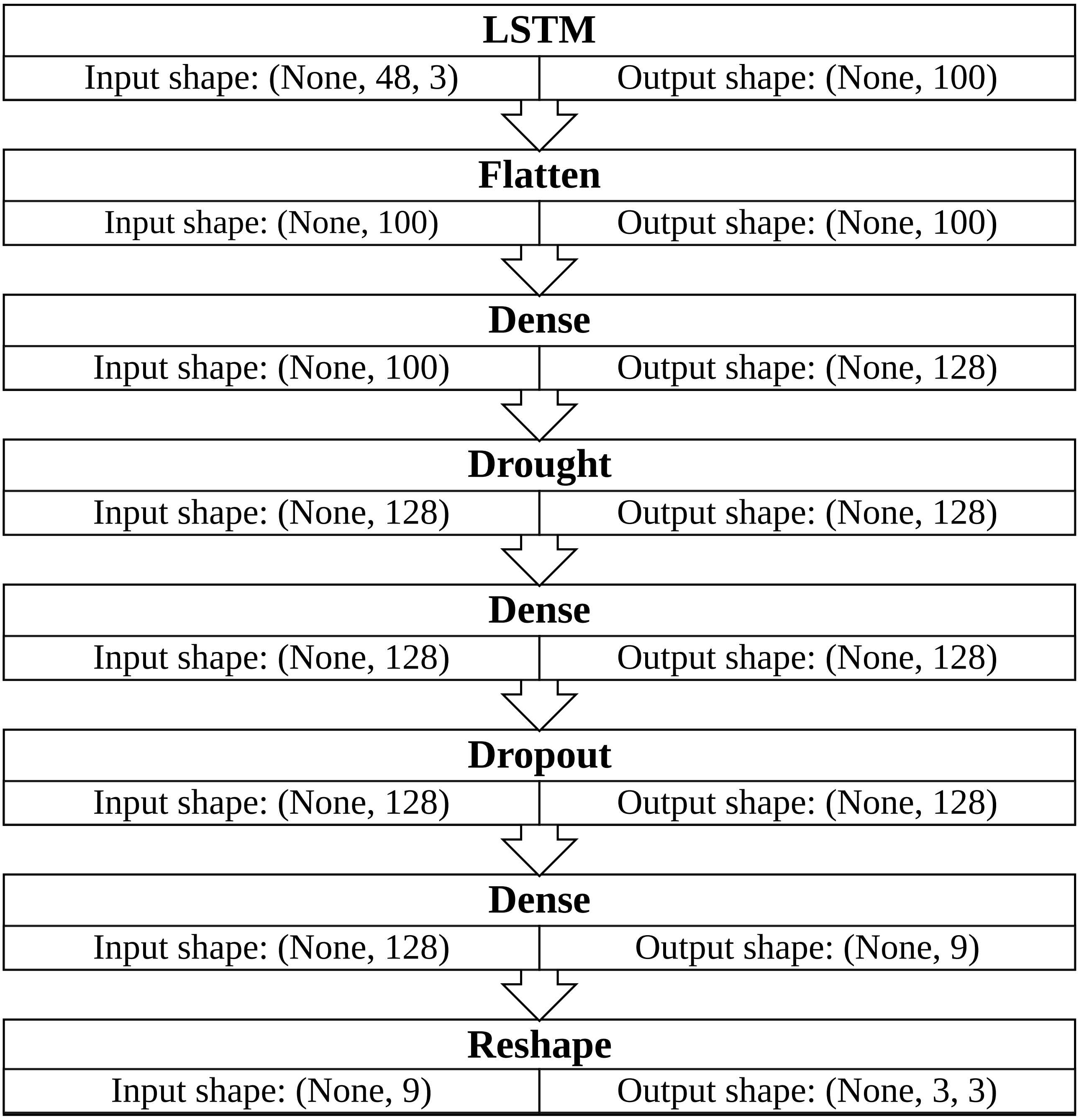

Figure 11: Vanilla LSTM Model component

The Stacked LSTM model enhances the Vanilla LSTM by stacking multiple LSTM layers to capture more complex patterns. It starts with an LSTM layer with 150 units, followed by another with 100 units, and a final LSTM layer with 50 units. Each LSTM layer processes the sequential data, with the output from one layer serving as the input to the next. After the LSTM layers, the model includes flatten and Dense layers, similar to the Vanilla LSTM, to produce the final output.

The Bidirectional LSTM model processes the input sequence in both for- ward and backward directions, capturing dependencies from both directions. This model includes a single Bidirectional LSTM layer with 100 units. The bidirectional approach enhances the model's ability to understand context from both past and future data points within the sequence. The output from the Bidirectional LSTM layer is then flattened and passed through dense layers with Dropout to generate the final prediction.

The Stacked Bidirectional LSTM combines the strengths of bidirectional processing with multiple LSTM layers. It starts with a Bidirectional LSTM layer with 100 units, followed by another Bidirectional LSTM layer with 50 units. This configuration allows the model to capture complex temporal patterns from both directions. Similar to the other models, the output is flattened and processed through dense layers with Dropout to produce the final output.

The CNN-LSTM model integrates convolutional layers with LSTM layers to capture spatial and temporal dependencies. It begins with an input layer, followed by time-distributed Conv1D layers with 64 filters and a kernel size of 1, which apply convolution operations across the input sequences. A Time Distributed Max Pool- ing1D layer reduces the spatial dimensions, followed by a Time Distributed Flatten layer to prepare the data for the LSTM layer. A single LSTM layer with 50 units processes the temporal dependencies, followed by Flatten and Dense layers with Dropout to produce the final prediction.

The ConvLSTM model employs ConvLSTM2D layers to capture spatiotemporal dependencies directly. It starts with an input layer, followed by a ConvL-STM2D layer with 64 filters and a kernel size of (1, 2), which applies convolution and LSTM operations simultaneously. The output is flattened and passed through dense layers with Dropout to generate the final prediction. These models are compiled using the Adam optimizer and Mean Squared Error (MSE) as the loss function. The inclusion of Dropout layers in the dense sections of the models helps mitigate over fitting.

CHAPTER FOUR

4. RESULT AND DISCUSSION

4.1. Model Evaluation

The results are presented in the table 3. Compare the performance of various LSTM- based models in predicting drought conditions using the Precipitation at different timescales (3, 6, 9, 12, and 24 months). The performance metrics considered are Accuracy, Precision, Recall, and F1-Score.

Vanilla LSTM model demonstrates robust performance across all SPEI timescales, maintaining relatively high scores in Accuracy, Precision, Recall, and F1-Score. For SPEI3, it achieves an Accuracy and F1-Score of 0.80, indicating strong short-term predictive capabilities. However, as the timescale extends to SPEI-24, the performance slightly declines, with an Accuracy of 0.65 And an F1-Score of 0.66. This decline suggests that while Vanilla LSTM is effective for short-term predictions, its performance diminishes for longer- term forecasts.

Stacked LSTM model exhibits a different trend, with significantly lower performance metrics across all timescales. For instance, the Accuracy for SPEI-3 is only 0.40, and it gradually improves to 0.47 for SPEI-24. Similarly, the F1-Score starts at 0.42 for SPEI-3 and reaches 0.47 for SPEI-24.This indicates that the Stacked LSTM model struggles with both short-term and long-term predictions, we believe the reason is over fitting or insufficient learning of temporal dependencies.

Bidirectional LSTM model shows strong performance for short-term predictions, with an Accuracy of 0.76 and an F1-Score of 0.76 for SPEI-3. However, the performance declines significantly for longer timescales, with an Accuracy of 0.55 and an F1-Score of 0.56 for SPEI-24. This pattern suggests that Bi-LSTM is effective at capturing short-term temporal dependencies but less so for longer-term dependencies.

Stacked Bidirectional LSTM model has moderate performance metrics, with an Accuracy of 0.73 and an F1-Score of 0.73 for SPEI-3. Similar to the Bi-LSTM model, its performance decreases for longer timescales, achieving an Accuracy and F1-Score of 0.54 for SPEI-24. This indicates that while stacking bidirectional layers provides some benefits, it still faces challenges in maintaining performance over longer prediction horizons.

CNN-LSTM model performs well for short-term predictions, with an Accuracy of 0.74 and an F1-Score of 0.74 for SPEI-3. However, its performance declines for longer timescales, with an Accuracy of 0.51 and an F1-Score of 0.52 For SPEI-24. This suggests that while the CNN component enhances short-term predictions, the model struggles to maintain accuracy for extended periods.

ConvLSTM model shows strong performance for short-term predictions, with an Accuracy and F1-Score of 0.77 for SPEI-3. Its performance declines for longer time scales, similar to other models, with an Accuracy of 0.53 and an F1-Score of 0.53 for SPEI-24. This indicates that ConvLSTM is effective at capturing complex patterns in short-term data but faces challenges with long- term predictions.

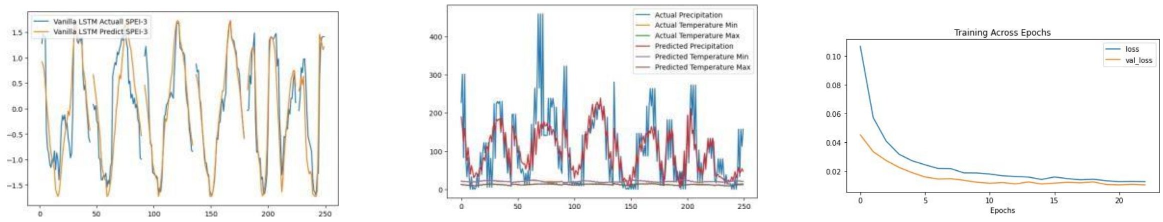

(a) SPEI-3 - Vanilla LSTM

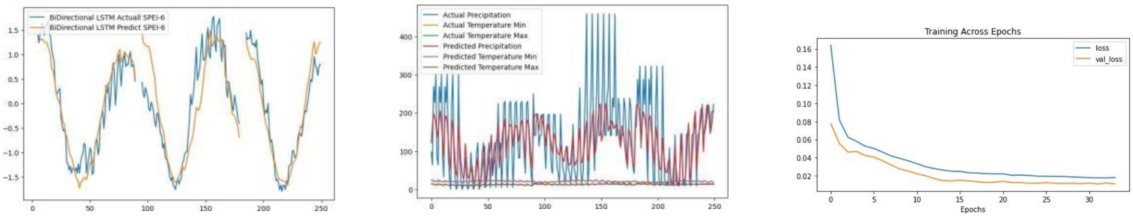

(b) SPEI-6 - BiDirectional LSTM

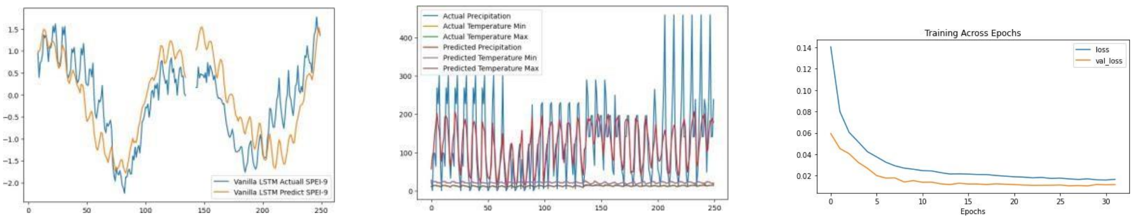

(c) SPEI-9 - Vanilla LSTM

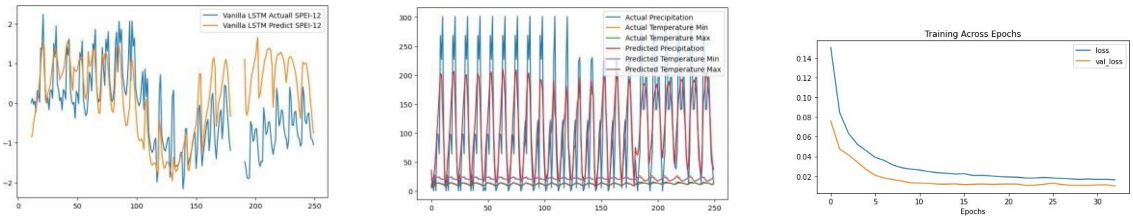

(d) SPEI-12 - Vanilla LSTM

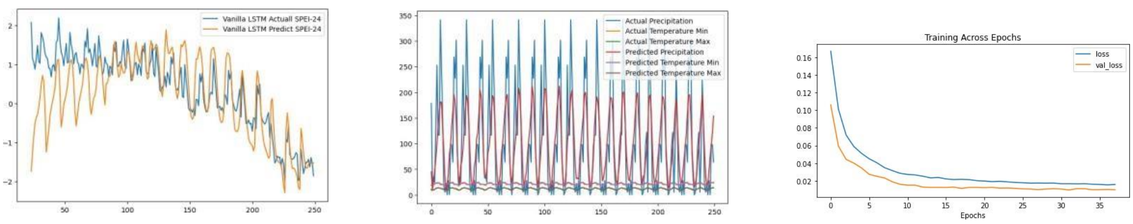

SPEI-24 - Vanilla LSTM

Figure 12: Model training result best from each season

4.2. Feature Directions

In the context of advancing drought prediction models, several avenues for future research and development can be explored. First, enhancing the model's ability to handle and integrate multisource data, including satellite imagery, soil moisture content, and other environmental variables, could significantly improve prediction accuracy.

This would involve developing hybrid models that combine the strengths of Convolutional Neural Networks (CNNs) for spatial data and Long Short-Term Memory (LSTM) networks for temporal data. There is potential in applying transfer learning techniques to leverage pre-trained models on larger, more diverse datasets, which could be fine-tuned for specific regional drought prediction. This approach would help in addressing the data scarcity issue in certain regions by utilizing knowledge from broader datasets.

Table 3: Model training result

Model	Metrics	SPEI-3	SPEI-6	SPEI-9	SPEI-12	SPEI-24
Vanilla LSTM	Accuracy	0.80	0.71	0.69	0.67	0.56
	Precision	0.80	0.71	0.69	0.68	0.58
	Recall	0.80	0.71	0.69	0.67	0.56
	F1-Score	0.80	0.71	0.69	0.68	0.67
Stacked LSTM	Accuracy	0.40	0.42	0.44	0.46	0.47
	Precision	0.44	0.39	0.41	0.46	0.48
	Recall	0.40	0.42	0.44	0.46	0.47
	F1-Score	0.42	0.41	0.42	0.46	0.47
	Accuracy	0.76	0.72	0.68	0.58	0.55
BiLSTM	Precision	0.77	0.71	0.69	0.59	0.56
	Recall	0.76	0.72	0.68	0.58	0.55
	F1-Score	0.76	0.71	0.68	0.58	0.56
Stacked	Accuracy	0.73	0.67	0.67	0.54	0.54
Bi-LSTM	Precision	0.74	0.67	0.67	0.55	0.55
	Recall	0.73	0.67	0.67	0.54	0.54

	F1-Score	0.73	0.67	0.67	0.54	0.54
CNN - LSTM	Accuracy	0.74	0.67	0.56	0.56	0.51
	Precision	0.75	0.68	0.55	0.56	0.52
	Recall	0.74	0.67	0.56	0.56	0.51
	F1-Score	0.74	0.67	0.55	0.56	0.52
ConvLSTM	Accuracy	0.77	0.71	0.66	0.54	0.53
	Precision	0.77	0.72	0.66	0.55	0.54
	Recall	0.77	0.71	0.66	0.54	0.53
	F1-Score	0.77	0.71	0.66	0.54	0.53

Moreover, the incorporation of real-time data assimilation methods can be beneficial. Implementing frameworks that can continuously update and refine the models with real-time data inputs would enhance their responsiveness and accuracy in dynamic environments.

Additionally, exploring the use of Generative Adversarial Networks (GANs) for synthetic data generation could provide a means to augment training datasets, thereby improving model robustness and performance. This technique could be particularly useful for simulating extreme weather events.

Further, integrating socio-economic factors and water resource management strategies into the predictive models can provide a more holistic view of drought impacts and facilitate more comprehensive mitigation planning. This interdisciplinary approach would ensure that predictions are not only accurate but also actionable.

We believe these future directions, the field of drought prediction can continue to evolve, providing more reliable and timely forecasts that are essential for mitigating the adverse impacts of droughts on communities and ecosystems.

Table 4: Prediction Result of the proposed Model in the coming five years for the selected area of Ethiopia.

No	**Year**	**Area/site**	**Prediction**	**Remark**
1	2025	Konso	$1.0 \leq SPEI < 1.5$	Moderately Wet
		Bahirdar,	$-1.0 < SPEI < 1.0$	Near Normal
		Diredawa,	$1.5 \leq SPEI < 2.0$	Very Wet
		Wachamo	$-1.0 < SPEI < 1.0$	Near Normal
		Bure	$-1.0 < SPEI < 1.0$	Near Normal
2	2026	Konso	$1.0 \leq SPEI < 1.5$	Moderately Wet
		Bahirdar,	$-1.0 < SPEI < 1.0$	Near Normal
		Diredawa,	$1.5 \leq SPEI < 2.0$	Very Wet
		Wachamo	$-1.0 < SPEI < 1.0$	Near Normal
		Bure	$-1.0 < SPEI < 1.0$	Near Normal
3	2027	Konso	$1.0 \leq SPEI < 1.5$	Moderately Wet
		Bahirdar,	$-1.0 < SPEI < 1.0$	Near Normal
		Diredawa,	$1.5 \leq SPEI < 2.0$	Very Wet
		Wachamo	$-1.0 < SPEI < 1.0$	Near Normal
		Bure	$-1.0 < SPEI < 1.0$	Near Normal
4	2028	Konso	$-1.5 \leq SPEI \leq -1.0$	Moderately Dry
		Bahirdar,	$1.0 \leq SPEI < 1.5$	Moderately Wet
		Diredawa,	$-1.0 < SPEI < 1.0$	Near Normal
		Wachamo	$1.5 \leq SPEI < 2.0$	Very Wet
		Bure	$-1.0 < SPEI < 1.0$	Near Normal
5	2028	Konso	$-1.0 < SPEI < 1.0$	Near Normal
		Bahirdar,	$1.0 \leq SPEI < 1.5$	Moderately Wet
		Diredawa,	$-1.0 < SPEI < 1.0$	Near Normal
		Wachamo	$1.5 \leq SPEI < 2.0$	Very Wet
		Bure	$-1.0 < SPEI < 1.0$	Near Normal

CHAPTER 5

CONCLUSION AND FUTURE WORKS

In this study, we explored the effectiveness of various LSTM-based models for drought prediction using the Standardized Precipitation Evapotranspiration Index (SPEI) at different timescales. The models evaluated include Vanilla LSTM, Stacked LSTM, Bidirectional LSTM, Stacked Bidirectional LSTM, CNN-LSTM, and Con- LSTM. Each model was assessed based on key performance metrics: Accuracy, Precision, Recall, and F1-Score. The results indicate that the Vanilla LSTM and ConvLSTM models perform best for short-term drought predictions, particularly for SPEI-3, with high scores in all metrics. These models effectively capture temporal dependencies and provide robust short-term forecasts. However, their performance declines as the prediction horizon extends to SPEI-24, highlighting a common challenge in long-term prediction accuracy. The Stacked LSTM model showed significantly lower performance across all timescales, suggesting potential issues with over fitting or insufficient temporal learning. The Bidirectional LSTM models performed well in capturing short-term dependencies but also faced a decline in long-term prediction accuracy. The CNN-LSTM model demonstrated the benefit of integrating spatial and temporal data for short- term predictions but struggled with long-term accuracy.

Overall, while each model has its strengths, there is a clear need for further refinement to improve long-term prediction capabilities. Future work should focus on integrating multi-source data, employing transfer learning, incorporating real-time data assimilation, and exploring synthetic data generation with GANs.

Additionally, an interdisciplinary approach that includes socio-economic factors and real-world validation can enhance the practical applicability of these models. By advancing these research directions, we can develop more accurate and reliable drought prediction models, providing essential tools for effective water resource management and mitigation strategies to combat the adverse impacts of droughts on communities and ecosystems.

In our current, we have used temperature, rainfall and precipitation. In our Future works, we will consider humidity, soil, wind and radiation. Moreover, apart from the current historical data, we will further explore on spatial, temporal and instantaneous data, which are critically needed by current drought prediction models.

REFERENCES

[1].Wilhite, D. A., & Glantz, M. H. (1985). Understanding the drought phenomenon: The role of definitions.*WaterInternational*, 10(3), 111–120. https://doi.org/10.1080/02508068508686328

[2].Adams, J. (2017). Climate indices: An open-source Python library providing reference implementations of commonlyused climate indices. URL: https://github.com/monocongo/climate_indices

[3].Belayneh, A., Adamowski, J., & Khalil, B. (2015). Short-term SPI drought forecasting in the Awash River Basin in Ethiopia using wavelet transforms and machine learning methods. *Sustainable Water Resources Management*, 2(1), 87–101. https://doi.org/10.1007/s40899-015-0040-5

[4].Belayneh, A., Adamowski, J., & Khalil, B. (2014). Long-term SPI drought forecasting in the Awash River Basin in Ethiopia using wavelet neural network and wavelet support vector regression models. *Journal of Hydrology*, 508, 418–429. https://doi.org/10.1016/j.jhydrol.2013.10.052

[5].Chaudhari, S. S., Sardar, V., & Ghosh, P. (2023). Drought classification and prediction with satellite image-based indices using variants of deep learning models. *International Journal of Information Technology*, 15(7), 3463–3472. https://doi.org/10.1007/s41870-023-01379-4

[6].Hochreiter, S., & Schmidhuber, J. (1997). Long Short-Term Memory. *Neural Computation*, 9(8), 1735–1780. https://doi.org/10.1162/neco.1997.9.8.1735

[7].Kheyruri, Y., Sharafati, A., & Neshat, A. (2023). Predicting agricultural drought using meteorological and ENSO parameters in different regions of Iran based on the LSTM model. *Stochastic Environmental Research and Risk Assessment*, 37(9), 3599–3613. https://doi.org/10.1007/s00477-023-02465-6

[8].Richman, M. B., Leslie, L. M., & Segele, Z. T. (2016). Classifying drought in Ethiopia using machine learning. *Procedia Computer Science*, 95, 229–236. https://doi.org/10.1016/j.procs.2016.09.319

[9].Svoboda, M. D., & Fuchs, B. A. (2016). Handbook of drought indicators and indices.

[10].UNICEF. (2024). The drought is driving up cases of child hunger and malnutrition in Borena. Retrieved from https://www.unicef.org/Ethiopia/stories/drought-drivingcases-child-hunger-and-malnutrition-borena

[11].Xu, D. et al. (2023). Application of a hybrid ARIMA-LSTM model based on the SPEI for drought forecasting. *Environmental Science and Pollution Research*.

[12].Bachmair, S., Stahl, K., Collins, K., Hannaford, J., Acreman, M., Svoboda, M.,
Knutson, C., Smith, K. H., Wall, N., Fuchs, B., Crossman, N. D., & Overton, I. C. (2016). Drought indicators revisited: The need for a wider consideration of environment and society. *Wiley Interdisciplinary Reviews: Water*, 3(4), 516–536. https://doi.org/10.1002/wat2.1154

[13].Wanders, N., van Lanen, H. A. J., & van Loon, A. F. (2010). Indicators for Drought Characterization on a Global Scale (Technical Report No. 24). Wageningen University and Research, 24, 1–93.

[14].Yihdego, Y., Vaheddoost, B., & Al-Weshah, R. A. (2019). Drought indices and indicators revisited. *Arabian Journal of Geosciences*, 12(3). https://doi.org/10.1007/s12517-019-4237-1

[15].Agana, N. A., & Homaifar, A. (2017). A Deep Learning Based Approach for LongTerm Drought Prediction. *Journal of Water Resources Planning and Management*.

[16]Nandgude, N., et al. (2023). Drought Prediction: A Comprehensive Review of Different Drought Prediction Models and Adopted Technologies. *Environmental Monitoring and Assessment*, 195(4).

[17].Wilhite, D. A., & Glantz, M. H. (1985). Understanding Drought Dynamics. *Water International*, 10(3), 111–120. https://doi.org/10.1080/02508068508686328

[18].Bachmair, S., et al. (2016). Drought Management Challenges. *Wiley Interdisciplinary Reviews: Water*, 3(4), 516–536. https://doi.org/10.1002/wat2.1154

[19].Drought Analysis in Hawaiʻi (1920-2019). (2020). *U.S. Geological Survey*.

[20].Mei, P. (2020). Deep Learning for Drought Prediction in Yunnan Province. *Journal of Hydrology*.

[21].Australian Bureau of Meteorology. (2010). *Australian climate variability and change: Drought*. Retrieved from https://www.bom.gov.au/climate/drought/

[22].State of California Department of Water Resources. (2017). *California's drought: An overview*. Retrieved from https://water.ca.gov/Programs/Drought

[23].United Nations Office for the Coordination of Humanitarian Affairs. (2011).
Drought: Causes, impacts, and responses. Retrieved from https://www.unocha.org/theme/drought World Bank. (2020). *Managing drought: Strategies and solutions*. Retrieved from ttps://www.worldbank.org/en/topic/waterscarcity/overvi